Electromagnetic Pulse Welded Aluminium to Copper Sheet Joints: Morphological and Mechanical Characterization

K. Faes[*], I. Kwee

Belgian Welding Institute, Belgium
[*]Corresponding author. Email: Koen.Faes@bil-ibs.be

Abstract

This study investigated joining of Al to Cu sheets by electromagnetic pulse welding, which is a solid-state welding process that uses electromagnetic forces to join materials. The interfacial morphology and mechanical properties of the Al/Cu joints were analysed and related to the welding process parameters. The centre section of the Al/Cu joints evolved from a non-welded to a welded zone. The welded zone started with a wavy interface, consisting of thick interfacial layers with defects and evolved to a relatively flat interface without an interfacial layer. Interfacial phases resulted from solid-state mechanical mixing and/or very localised interfacial heating. The interfacial layers had a thickness ranging from 2-39 μm, an interface waviness amplitude up to 11 μm and contained 31-75 wt% Cu. The interfacial layer thickness and the weld length are determined by both the discharge energy and the stand-off distance. A trade-off existed between a homogeneous interface and the maximum weld length when the stand-off distance is changed. The interfacial layer exhibited an increased hardness compared to Al and Cu. A higher tensile force, up to 4,9 kN, was achieved at a higher energy and a lower stand-off distance. One of the factors determining the tensile force was the width of the welded area.

Keywords

Welding, Sheet metal, Analysis

1   Introduction

Aluminium-copper (Al/Cu) hybrid parts, as a substitution for Cu parts, result in both weight and cost reduction, and are highly relevant in numerous applications related to the electrical, heating and cooling sector (Bergmann et al., 2013; Abbasi et al., 2001).

However, Al to Cu joined by thermal welding processes presents challenges for achieving a good joint quality, due to their highly dissimilar mechanical and thermal properties, which can result in large stress gradients during heating. In contrast, electromagnetic pulse welding is a solid-state welding technology that uses electromagnetic forces to join the materials. In this process, a power supply is used to charge a capacitor bank. When the required amount of energy is stored in the capacitors, it is instantaneously released into a coil, during a very short period of time. The discharge current induces a strong transient magnetic field in the coil, which generates a magnetic pressure that causes one workpiece to impact with another workpiece. Under the correct circumstances, this leads to an atomic bond between the two metal workpieces, in either a tubular or sheet configuration. The objective of the present work is to investigate electromagnetic pulse welding of Al to Cu sheets achieved at different welding conditions. The weld interface and mechanical properties of the resulting Al/Cu sheet joints are analysed and related to the welding process parameters, namely the discharge energy, the stand-off distance, and the overlap between the coil and the Al sheet.

2 Experimental Procedure

2.1 Set-up of the Electromagnetic Pulse Welding Process

Electromagnetic pulse sheet welding of Al 1050 H14 (sheet dimensions: 50 mm x 50 mm x 1 mm and 48 mm x 50 mm x 1 mm) to Cu (sheet dimensions: 67 mm x 50 mm x 1 mm) sheets was performed using a Pulsar model 50/25 system with a maximum charging energy of 50 kJ (corresponding with a maximum capacitor charging voltage of 25 kV). The total capacitance of the capacitor banks equals 160 μF. Figure 1 shows the overlap configuration of the Al sheet and Cu sheet in the flat coil. The Al sheet is called the flyer sheet and is located on top of the coil conductor. The Cu sheet is called the parent sheet. The stand-off distance is the distance by which the Al flyer sheet is separated from the Cu parent sheet prior to discharge. The overlap is the overlap distance between the flat coil and the Al flyer sheet. The free length is the part of the Al flyer sheet that is being accelerated.
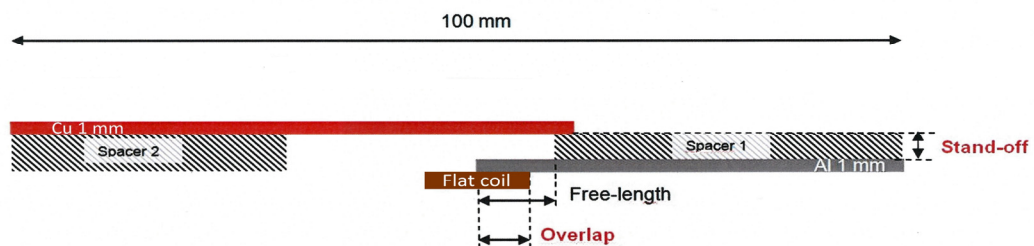

Figure 1: Overlap welding configuration of the Al flyer sheet and Cu parent sheet

2.2 Electromagnetic Pulse Sheet Welding Conditions

An overview of the selected welding parameters is shown in Table 1. In total, 27 different welding conditions were tested. The discharge energy, stand-off distance and overlap distance were varied, whereas the free length was fixed throughout all experiments.

Discharge energy [kJ]	Stand-off distance [mm]	Overlap distance between the flat coil and Al flyer sheet [mm]	Free length [mm]
10, 12, 14, 16, 18	2, 3, 4	8, 10	15

Table 1: Selected parameters for electromagnetic sheet welding of Al to Cu sheets

2.3 Weld Characterization

The interfacial morphology and the weld length were assessed by optical microscopy (OM) and Field Emission Scanning Electron Microscopy (SEM). Energy-Dispersive X-ray Spectroscopy (EDX) analysis was conducted to semi-quantitatively identify the chemical composition of the interfacial layer. Subsequently, hardness traverses (micro hardness testing; weight 5,0 gram) and tensile tests were performed.

3 Results & Discussion

3.1 Weld Interface

Figure 2 (left) shows a typical Al/Cu sheet weld and Figure 2 (right) a typical metallographic cross-section obtained at the centre of the weld. The first impact is at the right extremity of the Al flyer sheet, after which the weld formation advances to the left. In general, all metallographic cross-sections show that Al/Cu sheet joints evolve from a non-welded zone to a welded zone. The weld length corresponds to the length of the welded zone.
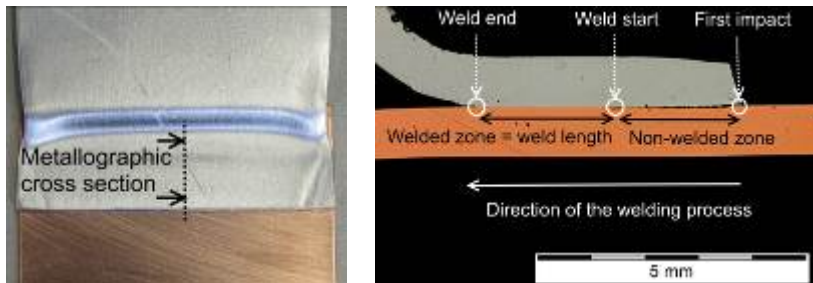

Figure 2 (left): As-welded Al/Cu sheets (discharge energy: 14 kJ, stand-off distance: 2 mm, overlap distance: 10 mm, free length: 15 mm) (right) Metallographic cross-section taken at the centre of the welded sample (discharge energy: 10 kJ, stand-off distance: 3 mm, overlap: 10 mm, free length: 15 mm)

Based on measurements and modelling studies performed by other authors, the evolution of the non-welded to the welded zone can be attributed to the evolution of pure normal Lorentz forces to a combination of normal and shear Lorentz forces (Schäfer and Pasquale; Kore et al., 2007; Kore et al., 2010), the increase of the impact angle (Watanabe et al., 2009) and the change of the impact velocity (Schäfer and Pasquale) during the welding process. The direction and the magnitude of the Lorentz force determine the impact angle between the flyer and parent sheet. The combination of the impact angle and the impact velocity is defined in the so-called welding window, which specifies the requirements of the impact velocity and the impact angle for welding to occur (Göbel et al., 2010; Watanabe et al., 2009; Kore et al., 2010). Under the correct conditions, a jetting

effect can then take place that effectively removes the oxides from the surfaces and allows for atomic bonding to occur (Watanabe et al., 2009).

3.2   Interfacial Morphology of the Welded Zone

Figure 3 shows a detailed view of the typical evolution of a welded zone (i.e. the central part of Figure 2, right). At first, a relatively flat interface with a small interfacial layer containing macrocracks and pores is observed (Figure 3a). Subsequently, the interface waviness amplitude, defined as the difference between the maximum and the minimum of a wave, and the thickness of the interfacial layer increase. The interfacial layer becomes strongly porous, with randomly dispersed porosities in different sizes. In addition, transverse microcracks, restricted to the interfacial layer, are noticed (Figure 3b). This is followed by a more homogeneous interfacial layer with a similar interfacial thickness but less porosities (Figure 3c). Further along the weld, the thickness of this homogeneous interfacial layer decreases (Figure 3d) and towards the end of the weld, a small wavy interface and thin interfacial layer without any defects is present (Figure 3e). Finally, the interface becomes relatively flat, without any visible interfacial layers (Figure 3f).
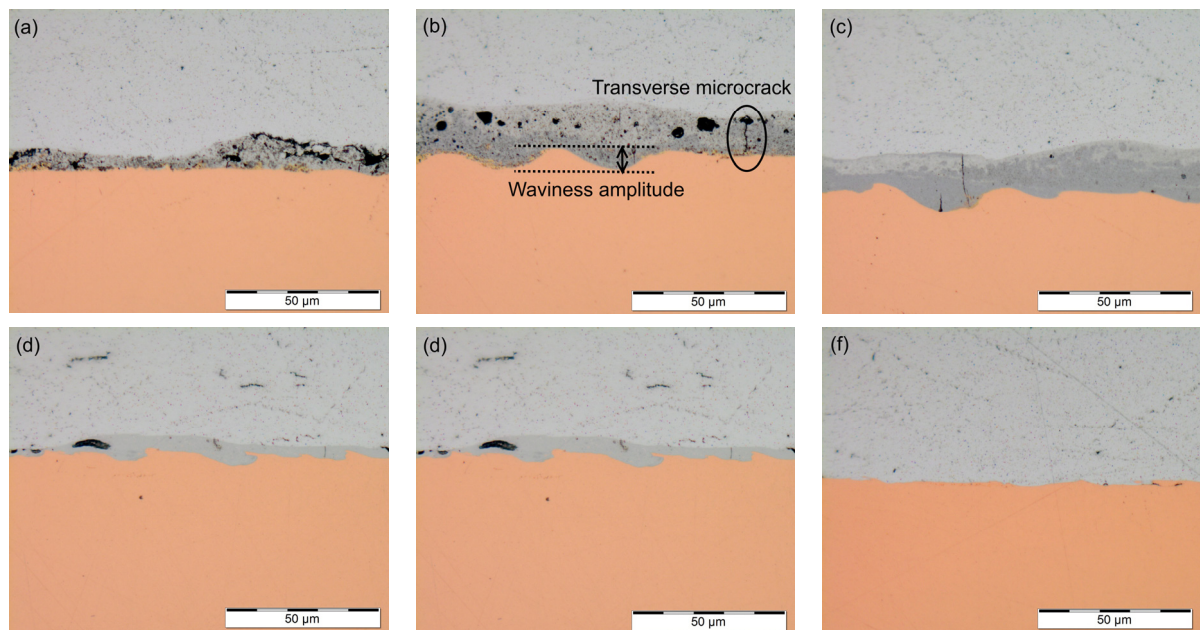

Figure 3: Evolution of a typical weld interface from the start (a) to the end (f) of the welded zone (from right to left in Figure 2) (discharge energy: 18 kJ, stand-off distance: 3 mm, overlap distance: 10 mm, free length: 15 mm)

Table 2 summarizes the wt% Cu, range of interfacial layer thickness, range of waviness amplitude, and defects present in the different interfacial layers of the welded zone.

Colour observed by optical microscopy	Position within the welded zone	%wt Cu	Interfacial layer thickness [µm]	Waviness amplitude [µm]	Defects
Light grey	Mainly at the weld end, sometimes also in the weld middle	≈31-41	2-10	< 6	No or small porosities
Dark grey, in combination with light grey	Weld middle & weld start	≈54-62	3-26	6-11	Medium-sized porosities, mainly transverse cracks
Brown, in combination with light grey and dark grey	Weld start	≈72-75	14-39	6-11	Large porosities, transverse and longitudinal cracks

Table 2: *Identification of the wt% Cu, range of interfacial layer thickness, range of waviness amplitude, and defects in the different interfacial layers of the welded zone*

The interfacial layers, found along the weld interface, can be formed by two mechanisms. Firstly, the interfacial phases are formed by solid-state mechanical mixing, during which severe local plastic deformation takes place (Sterb et al., 2010). Secondly, a local temperature rise and localised interfacial heating with subsequent fast cooling can result in interfacial layers (Göbel et al. 2010; Raoelison et al., 2012; Zhang et al., 2011). When using a large discharge energy, melting at the interface can also occur, followed by cooling and solidification shrinkage. Melting can be evidenced by the presence of spherical pores (Figure 4). Such a spherical pore reveals a molten and re-solidified area, which can be an indication that interfacial melting has taken place. In addition, spherical and irregular pores can originate from metallurgical preparations such as grinding and polishing.
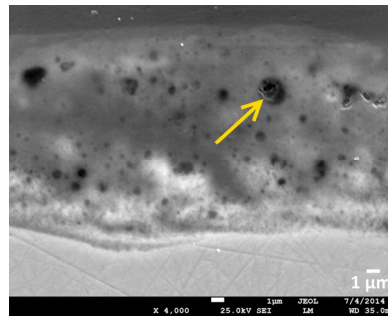

Figure 4: *Spherical pore within an interfacial layer, revealing a molten and re-solidified area that indicates that localized interfacial melting has occurred (discharge energy: 14 kJ, stand-off distance: 3 mm, overlap: 10 mm, free length: 15 mm)*

The change of the interfacial morphology within the welded zone can be attributed to the continuous variation of the impact velocity and impact angle during the welding process, as found in (Göbel et al., 2010; Göbel et al., 2011; Watanabe et al., 2009). The presence of a higher wt% Cu at the start and the middle of the welded zone possibly indicates that the impact energy at those locations is sufficient to allow more mechanical mixing of Cu with Al and more heating of the materials. In contrast, the presence of less wt% Cu towards the end of the welded zone may indicate that the impact energy decreases, promoting less mixing and less heating of the materials.

3.3 Effect of the Welding Process Parameters on the Interfacial Morphology and Weld Length

The thickness of the interfacial layer and hence its structural and chemical composition are determined by both the stand-off distance and the discharge energy. No effect of the overlap distance between the coil and the Al sheet was found in the present study.

At an overlap of 10 mm, a discharge energy of 16 kJ and a stand-off distance of 4 mm, the welded zone consists of a homogeneous weld interface with an interfacial thickness of 5 μm (Figure 5a). At the same overlap and discharge energy, but with a decreased stand-off distance of 3 mm, the welded zone consists of an inhomogeneous weld interface with a large interfacia0 thickness up to 25 μm, many porosities and several transverse microcracks (Figure 5b).

The change of the weld interface for a lower stand-off distance can be attributed to the larger impact velocity for a stand-off of 3 mm. When using a stand-off distance of 4 mm, it is likely that the velocity was already decreasing prior to impact, leading to a lower impact velocity compared to the situation when using a stand-off distance of 3 mm. For this reason, it was assumed that more kinetic energy is available for a stand-off distance of 3 mm that can be transformed into energy for bonding. In that case, also more localised interfacial heating can take place, as observed in (Marya et al., 2004), resulting in a larger interfacial layer thickness.

A similar observation is found for the effect of the discharge energy on the interfacial layer thickness. At the same overlap and stand-off distance, but at a higher discharge energy, the interfacial layer thickness increases and contains more porosities and cracks.
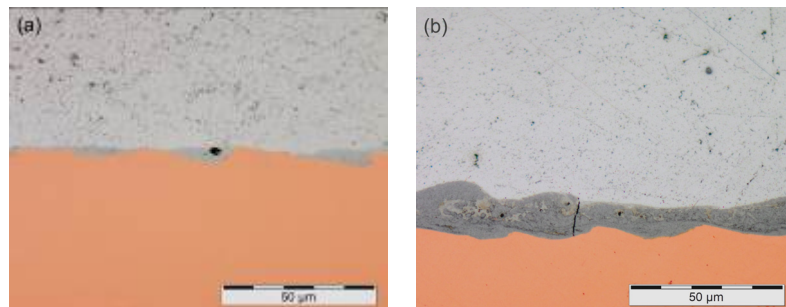

***Figure 5**: Effect of the stand-off distance on the welded zone, obtained with: discharge energy 16 kJ, overlap distance: 10 mm, free length: 15 mm (a) stand-off distance: 4 mm, interfacial thickness: 5 μm (b) stand-off distance: 3 mm, interfacial thickness: 20 μm*

Figure 6 shows the weld length as a function of the discharge energy, for the different combinations of overlap and stand-off distances. Also the weld length is determined by both the stand-off distance and the discharge energy. The maximum weld length is obtained at the optimal stand-off distance of 3 mm, at which the impact velocity and impact angle are situated in a range of the welding window that allows for a maximum jetting effect and hence a maximum weld length. In contrast, the minimum weld length is obtained at a stand-off distance of 2 mm, which indicates that this distance is too small since at the time of impact, the Al flyer sheet has not accelerated yet up to the correct impact velocity. Hence, the impact energy is insufficient to initiate bonding. Medium weld lengths are obtained at a stand-off distance of 4 mm, which indicates that this stand-off

distance is too large, since prior to impact the impact velocity has probably already started to decrease, as discussed previously. A similar observation is found for the effect of the discharge energy on the weld length. At the same overlap and stand-off distance, the maximum weld length is obtained at a discharge energy of 16 kJ, above and below which the weld length decreases.
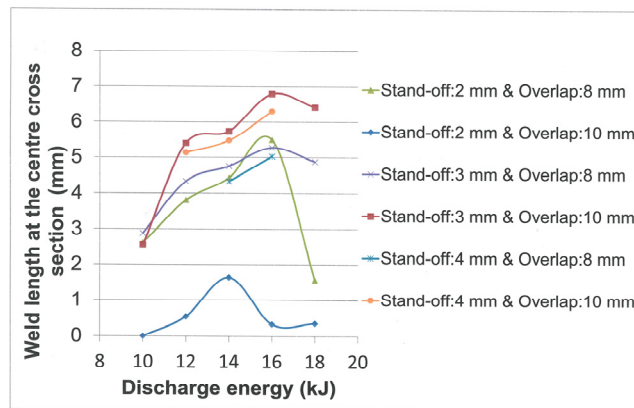

Figure 6: *Weld length at the centre cross section as a function of the discharge energy for different combinations of the stand-off distance (2-3-4 mm) and the overlap distance (8-10 mm)*

A trade-off exists between a homogeneous interface and a maximum weld length. By decreasing the stand-off distance from 4 to 3 mm, there is change from a homogeneous weld interface with a small interfacial layer thickness to an inhomogeneous interface with a larger interfacial layer thickness (Figure 5) and an increase of the weld length from 6,3 to 6,8 mm (Figure 6). This can possibly be attributed to a higher impact velocity achieved at the stand-off distance equal to 3 mm, which results in more kinetic energy available to be transformed into energy for bonding. As a result, a longer weld length is achieved but also more mechanical mixing, more interfacial heating, which lead to an inhomogeneous interface with a larger interfacial layer thickness.

3.4 Mechanical Characteristics

3.4.1 Hardness

Figure 7 shows a hardness traverse across an Al/Cu weld interface. The interfacial layer has a higher hardness (370,8 HV) compared to the base materials Al (average hardness 25,8 HV) and Cu (average hardness 52,3 HV). This increase of the hardness can confirm that phase transformations have taken place.
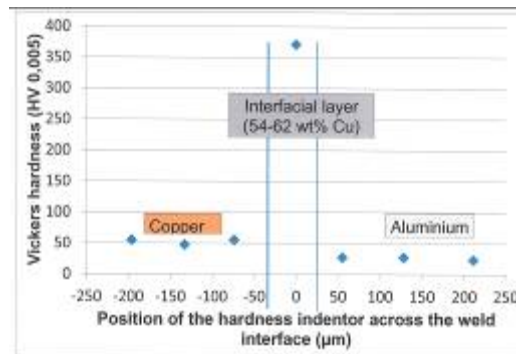
Figure 7: *Vickers hardness traverse across an Al-Cu weld interface (discharge energy 16 kJ; stand-off distance: 3 mm, overlap distance: 8 mm, free length: 15 mm)*

3.4.2 Tensile Force

Figure 8 shows the tensile force as a function of the discharge energy, for different combinations of the stand-off distance and overlap distance. A higher tensile force is achieved at a higher discharge energy and at a lower stand-off distance. Therefore, although energies higher than 10 kJ generally result in a larger interfacial thickness and a larger amount of defects within, the increase of the tensile force at a higher discharge energy shows that the presence of interfacial phases do not necessarily degrade the welds. Instead, interfacial phases can possibly provide additional strength due to their increased hardness compared to the base material. For most welding conditions, the welds with a higher tensile force (4-4,8 kN) have a large interfacial layer thickness (14 to 21 μm), whereas the welds with a lower tensile force (3-4 kN) have a small interfacial layer thickness (4 to 14 μm). The exception are welds obtained at a stand-off distance of 2 mm and an overlap of 10 mm, where all welds exhibit a higher tensile force (4-4,6 kN), but contain a small interfacial thickness (2 to 15 μm).
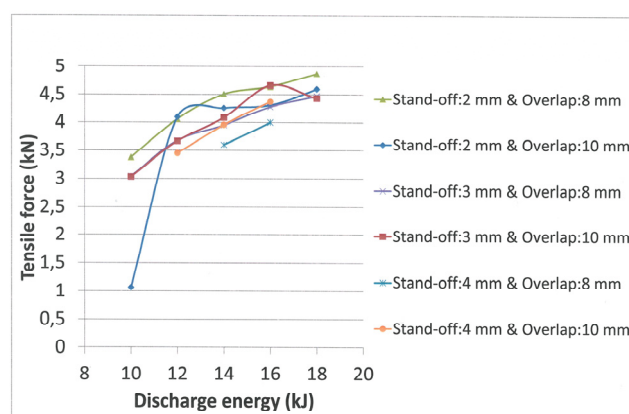

Figure 8: *Tensile force as a function of the discharge energy for different combinations of the stand-off distance (2-3-4 mm) and the overlap distance (8-10 mm)*

A higher tensile force is achieved for a larger weld width (Figure 9). An increase of the weld width is similarly achieved at a higher discharge energy and a lower stand-off distance of 2 mm. Therefore, the weld width is one of the main factors that determines the

tensile force that the weld can attain. No relation is found between the tensile force and the weld length at the centre of the weld.
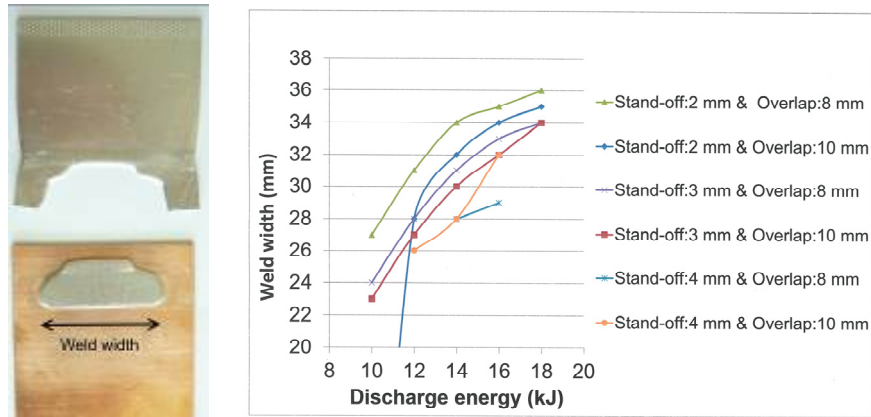

Figure 9*: (left) Al/Cu weld after tensile testing, showing the weld width (right) Weld width as a function of the discharge energy for different combinations of the stand-off distance (2-3-4 mm) and the overlap distance (8-10 mm)*

4   Conclusions

Al to Cu sheets are joined by the electromagnetic pulse technology using different welding conditions. The following conclusions can be drawn from the present experimental study:

− The centre of the Al/Cu sheet joints evolve from a non-welded zone to a welded zone. Based on measurements and modelling studies performed by other authors, this can be explained by the evolution of the direction and magnitude of the Lorentz forces, the change of the impact angle and the change of the impact velocity.
− Interfacial layers along the weld interface can be formed by solid-state mechanical mixing and/or by localised interfacial heating. The welded zone evolves from a thick and wavy interface with defects to a relatively flat interface without visible interfacial phases and defects. The interfacial layer thickness and the weld length are determined by both the discharge energy and the stand-off distance. A trade-off exists between a homogeneous interface with a small interfacial layer thickness and a maximum weld length.
− Higher tensile forces are obtained at a higher discharge energy and at a lower stand-off distance and weld width. The presence of interfacial layers can possibly provide additional tensile strength, due to their increased hardness.

Acknowledgements

References

Abbasi M., Karimi Taheri A., Salehi M.T., 2001. *Growth rate of interfacial compounds in Al/Cu bimetal produced by cold roll welding process.* Journal of Alloys Compounds 319, pp. 233-241.

Bergmann, J.P., Petzoldt F., Schürer R. Schneider S., 2013. *Solid-state welding of aluminium to copper-case studies.* Welding in the World 57, pp. 541-550.

Doley J.K., Kore S.D., 2011. Study of impact behavior of sheets in electromagnetic pulse welding. In: The 64th Annual Assembly of the International Institute of Welding, Chennai, India. The Indian Institute of Welding, CD-ROM Edition.

Göbel G., Beyer E., Kaspar J., Brenner B., 2011. Dissimilar metal joining: Macro-and Microscopic Effects of MPW. In: Proceedings of the 5th International Conference on High Speed Forming, Dortmund, Germany, pp. 179-188.

Göbel G., Kaspar J., Herrmannsdörfer T., Brenner B., Beyer E., 2010. Insights into interfacial phases on pulse welded dissimilar metal joints. In: Proceedings of the 4th International Conference on High Speed Forming, OH, USA, pp.127-136.

Kore S.D., Date P.P., Kulkarni S.V.,2007. *Effect of process parameters on electromagnetic impact welding of aluminium sheets.* International Journal of Impact Engineering 34, pp.1327-1341.

Kore S.D., Dhanesh P., Kulkarni S.V., Date P.P., 2010. *Numerical modeling of electromagnetic welding.* International Journal of Applied Electromagnetics 32, pp.1-19.

Marya M, Marya S, Priem D., 2004. On the Characteristics of Electromagnetic Welds between Aluminium and Other Metals and Alloys. In: The 57th annual Assembly of the International Institute of Welding, Osaka, Japan.

Raoelison R., Rachik M., Buiron N., Haye D., Morel M., Dos Santos B., Jouaffre D., Franz G., 2012. Assessment of gap and charging voltage influence on mechanical behavior of joints obtained by magnetic pulse welding. In: Proceedings of the 5th International Conference on High Speed Forming, Dortmund, Germany, pp.207-216.

Schäfer R., Pasquale P. *Material hybrid joining of sheet metals by electromagnetic pulse technology.* PST products GmbH, Alzenau, Germany; available at http://www.pstproducts.com/EMPT_sheetwelding_PSTproducts.pdf (accessed 18 January 2016).

Sterb A., Shribman V., Ben-Artzy A., Aizenshtein M., 2014. *Interface phenomena and bonding mechanism in magnetic pulse welding.* Journal of Material Engineering Performance 23, pp.3449-3458.

Watanabe M., Kumai S., 2009. *Interfacial morphology of magnetic pulse welded aluminium/aluminium and copper/copper lap joints.* Materials Transactions 50, pp. 286-292.

Watanabe M., Kumai S., 2009. *High-speed deformation and collision behavior of pure aluminium plates in magnetic pulse welding.* Materials Transactions 50, pp. 2035-2042.

Zhang Y., Suresh Babu S., Prothe C., Blakely M., Kwasegroch J., LaHa M., Daehn G., 2011. *Application of high velocity impact welding at varied different length scales.* Journal of Material Processing Technology 21, pp. 944-985.